LM-00K082
September 17, 2000

The Effects of Test Temperature, Temper, and Alloyed Copper on the Hydrogen-Controlled Crack Growth Rate of an Al-Zn-Mg-(Cu) Alloy

G.A. Young, Jr., J.R. Scully

The Effects of Test Temperature, Temper, and Alloyed Copper on the Hydrogen-Controlled Crack Growth Rate of an Al-Zn-Mg-(Cu) Alloy

George A. Young Jr.* and John R. Scully
Department of Materials Science and Engineering
Center for Electrochemical Science and Engineering
University of Virginia
Charlottesville, VA 22903-2442

*Current Address: Knolls Atomic Power Laboratory
P.O. Box 1072, Schenectady, NY 12301

ABSTRACT

The hydrogen embrittlement controlled stage II crack growth rate of AA 7050 (6.09 wt.% Zn, 2.14 wt.% Mg, 2.19 wt.% Cu) was investigated as a function of temper and alloyed copper level in a humid air environment at various temperatures. Three tempers representing the underaged, peak aged, and overaged conditions were tested in 90% relative humidity (RH) air at temperatures between 25 and 90 °C. At all test temperatures, an increased degree of aging (from underaged to overaged) produced slower stage II crack growth rates. The stage II crack growth rate of each alloy and temper displayed Arrhenius-type temperature dependence with activation energies between 58 and 99 kJ/mol. For both the normal copper and low copper alloys, the fracture path was predominately intergranular at all test temperatures (25-90 °C) in each temper investigated.

Comparison of the stage II crack growth rates for normal (2.19 wt.%) and low (0.06 wt.%) copper alloys in the peak aged and overaged tempers showed the beneficial effect of copper additions on stage II crack growth rate in humid air. In the 2.19 wt.% copper alloy, the significant decrease (~10 times at 25 °C) in stage II crack growth rate upon overaging is attributed to an increase in the apparent activation energy for crack growth. In the 0.06 wt.% copper alloy, overaging did not increase the activation energy for crack growth but did lower the pre-exponential factor, v_0, resulting in a modest (~2.5 times at 25 °C) decrease in crack growth rate. These results indicate that alloyed copper and thermal aging affect the kinetic factors that govern stage II crack growth rate. Overaged, copper bearing alloys are not intrinsically immune to hydrogen environment assisted cracking but are more resistant due to an increased apparent activation energy for stage II crack growth.

BACKGROUND

Hydrogen Controlled Crack Growth in Al-Zn-Mg-(Cu) Alloys

Precipitation hardened Al-Zn-Mg-(Cu) alloys are susceptible to intergranular environmentally assisted cracking (EAC) when exposed to wet gaseous environments [1-7]. Crack growth kinetics in moist gases are controlled by the relative humidity (RH) level, independent of the gas composition as shown by Hyatt and Speidel [1, 2]. Dry molecular gases such as hydrogen (H_2), oxygen (O_2), nitrogen (N_2), and air (~78% N_2, 21% O_2) do not initiate or support EAC crack growth. However, EAC readily initiates and propagates when precracked specimens loaded to near K_{IC} are exposed to wet gases. [1, 2]. In contrast to molecular hydrogen gas, intergranular cracking in 7XXX series alloys has also been observed in ionized hydrogen gas [8]. Since molecular hydrogen gas does not readily dissociate on 7XXX series alloy surfaces [8], ionizing likely promotes hydrogen uptake [9]. These results indicate that internally dissolved hydrogen is embrittling to 7XXX series aluminum alloys.

The water vapor content of gases has a limited effect on stage I of the crack velocity vs. stress intensity (or "*v-K*"), curve but stage II crack growth depends linearly on the water vapor pressure in Al-Zn-Mg alloys [1, 2]. Crack growth is observed at low relative humidities, where water condensation is unlikely at the crack tip and hydrogen embrittlement is implicated as the embrittlement mechanism [1, 2]. The linear dependence of crack growth rate on relative humidity from ~1-99%[1] indicates that the crack tip is not filled with condensed water and metal dissolution does not control crack growth at relative humidities ≤ 99%. Instead, the reaction of

[1] Note that Wei *et al.* interpret the data of Speidel and Hyatt in a different manner [10]. These researchers suggest a discontinuity in crack growth rate at approximately 60% RH, indicative of the condensation of water at the crack tip. However, condensation at 60% relative humidity does not agree with theoretical calculations using the Kelvin equation to predict condensation at a blunted crack tip nor with Speidel and Hyatt's interpretation of their own data.

aluminum with water vapor to produce high fugacity hydrogen gas is thought to control EAC of Al-Zn-Mg-(Cu) alloys via hydrogen embrittlement (see Equation 1 where X is the degree of hydration) [1, 2] and cracking in humid air is more accurately described as *hydrogen* environment assisted cracking (HEAC).

$$2Al(s) + (3+X)H_2O(g) \rightarrow Al_2O_3 \cdot X(H_2O)(s) + 3H_2(g) \quad \textbf{(1)}$$

The theoretical fugacity of hydrogen produced in Equation 1 can be estimated from the free energy change of the reaction ($\Delta G_{reaction}$) as shown in Equation 2 where R is the gas constant, T is the temperature, $K_{equilibium}$ is the reaction constant, f_{H_2} is the fugacity of hydrogen and f_{H_2O} is the fugacity of water vapor [11, 12].

$$\Delta G_{reaction} = -RT \ln K_{equilibrium} \approx -RT \ln\left(f_{H_2} / f_{H_2O}\right) \quad \textbf{(2)}$$

At 25 °C for the formation of boehmite ($Al_2O_3 \cdot H_2O$), $\Delta G_{reaction} \approx 1.1 \times 10^3$ kJ/mol and f_{H_2O} = 3169 Pa @ 25 yielding $f_{H_2} \approx 6 \times 10^{67}$ Pa or **10^{62} atm**! [13]. Clearly, there is a strong thermodynamic driving force for hydrogen production and entry when bare aluminum is exposed to humid air [11, 12].

Although the overall reaction shown in Equation (1) depicts H_2 gas production, water reduction at the oxide metal interface produces atomic hydrogen, which can be absorbed into the metal or recombine to form H_2 gas. It is the production of atomic hydrogen (Equation 3) which

makes water vapor such an aggressive environment for 7XXX series alloys. The production rate of hydrogen gas is high on the bare metal surface and decays via inverse logarithmic-type kinetics as surface films form [14].

$$H_2O + e^- \rightarrow (OH)^- + H \qquad (3)$$

The reaction between aluminum and water vapor (Equation 1) occurs spontaneously on bare aluminum and follows inverse logarithmic-type growth kinetics [15]. Theoretical calculations indicate that the thermodynamic fugacity of hydrogen produced in Equation (1) is on the order of ~10^{60} atm [11, 12]. Even though the theoretical fugacity of H production governed by Equation 1 is high, hydrogen production and uptake rates are temperature dependent. Increasing the temperature increases both the reaction rate of Equation 1 and, therefore, the rate of hydrogen production. Moreover, it increases the diffusivity of hydrogen into the metal [16]. Experimental investigation of near crack wake hydrogen concentrations confirms the thermodynamic calculations [14, 17]. They show greatly increased hydrogen levels in HEAC regions relative to the fast fracture region [14, 17].

Additional evidence that supports a HEAC mechanism in humid air comes from analysis of the Kelvin equation. The Kelvin equation (Equation 4) is used to predict the condensation of water over curved surfaces [18] where γ_{H_2O} is the surface tension of water, ρ_l and ρ_g are the densities of the liquid and vapor, r_c is the radius of the curved surface, R is the gas constant, T the temperature, M_{H_2O} the molecular weight of water, and $p_{vapor}/p_{saturation}$ the ratio of the pressure of the vapor to the saturation pressure of the vapor (See Table 1).

$$r_c = \frac{2\,\gamma_{H_2O}\,M_{H_2O}}{(\rho_l - \rho_g)\,RT\,ln\left(P_{vapor}/P_{saturation}\right)} \qquad (4)$$

Comparison of the radius required for condensation, r_c, (Equation 4) with the crack tip radius, r_{tip}, (Equation 5) over the temperature range 25-90 °C at the 90% RH level investigated in this study yields a required value r_c~10 nm for capillary condensation to occur. This required radius for condensation is approximately 100 times smaller than the calculated crack tip radius of AA 7050. The blunted crack tip radius was calculated from the work of Shih (Equation 5) where d_n is a parameter tabulated by Shih, K is the applied stress intensity factor, ν is Poisson's ratio, E is Young's modulus and σ_{flow} is the flow stress [19] (Table 2). Of course, these theoretical predictions must be used with caution since the actual crack tip likely contains physical irregularities and asperities which promote condensation.

$$r_{tip} = \frac{d_n\,K^2\left(1-\nu^2\right)}{2\,E\,\sigma_{flow}} \qquad (5)$$

This analysis further supports the notion that EAC in humid air is governed by hydrogen embrittlement and not anodic dissolution because a bulk aqueous phase is not expected over a broad range in RH levels where cracking is observed. Without the presence of bulk water at the crack tip (*i.e.*, enough adsorbed water to achieve the conductivity of bulk water), electrochemical reaction rates are significantly lowered [20] and are unable to achieve the current densities required to support the observed stage II crack growth rates (as high as ~27 amp/cm^2 for a crack growth rate of 10^{-3} mm/sec).

Influence of Metallurgical Factors on EAC

While Hyatt and Speidel showed the importance of water vapor in the HEAC of Al-Zn-Mg alloys and established an empirical correlation between aging time and *aqueous* EAC resistance, the effects of many metallurgical variables on *hydrogen* environment assisted cracking in Al-Zn-Mg-(Cu) alloys are poorly understood. Although the aqueous tensile testing of Al-Zn-Mg alloys under cathodic polarization suggests that the dependence of HEAC resistance on temper is the same as that for aqueous testing {*i.e.*, underaged (UA) < peak aged (PA) < overaged (OA)} [21-24], this relationship has not been confirmed for stage II crack growth rate in a modern Al-Zn-Mg-Cu alloy (*e.g.*, AA 7050) under HEAC control. Understanding the processes by which tempering affects HEAC resistance is an important step in defining the mechanism of crack advance and developing strategies to mitigate HEAC or improve HEAC resistance in high strength (near peak aged) tempers. The increase in EAC/HEAC resistance with aging time is accompanied by complex metallurgical changes that include:

- *Phase transformations (e.g., Gunier-Preston (G.P.) zones → η′→ η)*

  As 7XXX series alloys are heat-treated from the underaged condition to the overaged condition the strengthening precipitates evolve from the coherent G.P. zones to semicoherent η′, to incoherent η. This microstructural evolution affects several parameters that may be critical to EAC resistance including strength, ductility, slip mode, elemental segregation, electrochemical potential, hydrogen solubility, diffusivity, and trapping.

- *A change in strengthening mode from particle shearing to Orowan bypassing* [25]. Correlation of slip mode with EAC susceptibility suggests that planar slip exacerbates EAC while wavy slip (*i.e.*, particle looping) increases EAC resistance. The beneficial effects of copper may, in part, be explained by its ability to substitute into the strengthening precipitates $\{Mg(Zn_2) \rightarrow Mg(Cu, Zn)_2\}$ upon overaging and promote Orowan bypassing [21, 22, 26-28].

- *A change in precipitate size and distribution* [29, 30]. As the alloy is aged, both the intragranular and intergranular precipitate size and distributions change, as well as the precipitate free zone width and solute profiles. In general, overaging produces coarser, more widely spaced particles on both grain boundaries and in the grain interiors [31, 32].

- *A redistribution of alloying elements in the matrix, grain boundary region, and in the precipitates* [30, 33-37]. Redistribution of Mg, Zn, and Cu with tempering may affect EAC resistance as discussed below [30, 33-37].

The Effects of Chemical Segregation on Crack Growth

The presence or absence of alloying elements such as Mg, Zn, and Cu are important factors in EAC susceptibility since they can affect the microstructure and microchemistry of the grain boundary. Alloying elements can play a direct role in EAC resistance by altering the electrochemical potential of a region or a phase, as well as by influencing hydrogen uptake rates, solubility, and trapping. Since EAC in 7XXX-series alloys is predominantly intergranular, it is

possible that enrichment or depletion of Mg, Zn, and Cu or some other alloying element at the grain boundaries plays a critical role in the EAC resistance.

Magnesium segregation to grain boundaries may degrade EAC resistance by promoting grain boundary hydrogen uptake through MgO films [33, 38] or increase grain boundary hydrogen concentrations through the formation of a Mg-H complex [39, 40]. However, it is unclear whether or not these effects can be correlated with aging time (*i.e.*, EAC resistance). In a review of EAC of high strength aluminum alloys, Holroyd summarized available data for AA 7075, 7150, and 7050 and concluded that "free" grain boundary Mg (*i.e.*, Mg in solution, not $MgZn_2$ or other Mg containing precipitates) concentrations increase as the alloy is overaged [31, 35, 41]. This observation does not support the notion that EAC is controlled by Mg segregation given the known trend of increasing EAC resistance with increasing aging time. Similar to Mg, grain boundary enrichment of Zn has been hypothesized to exacerbate EAC by increasing the solubility of hydrogen at grain boundaries [42]. However, this interaction between hydrogen and Zn is unproven and Zn-H interactions may be weak [41].

While the precise effects of Mg and Zn on EAC resistance are poorly understood and the literature often conflicting, the beneficial effects of copper on EAC are well-established [43-47]. Many 7XXX series alloys contain on the order of 2 wt.% Cu to improve EAC resistance [43, 45, 48]. Empirically, it is known that EAC resistance in aqueous solution increases with the degree of overaging and with increased levels of alloyed copper [35, 41, 43, 45, 48].

Copper increases the supersaturation of the quenched alloy, which, during aging, increases the upper temperature limit of G.P. zone formation, providing additional nucleation sites for η' precipitation [29, 49]. Livak and Papazian have proposed that Cu-Mg-vacancy complexes form during quenching from the solution heat treat [50]. These vacancy rich clusters are thought to promote the nucleation rate of η' during aging and may facilitate copper incorporation into the precipitates. This description of the role of copper in the precipitation process is further supported by the transmission electron microscopy (TEM) and differential scanning calorimetry (DSC) work of Fujikawa *et al.* [51] and by the TEM work of Chinh [49] who observed copper rich G.P. zones in Al-Zn-Mg-Cu alloys. Copper bearing η' or η particles [30] may affect the EAC susceptibility of the alloy.

Note that the beneficial effects of overaging and copper additions have not been confirmed by testing under HEAC control. While there has been significant research into the effects of copper, [35, 41, 45, 48, 52] there is little agreement over the precise mechanisms by which overaging and alloyed copper increase EAC resistance. Proposed mechanisms by which copper and overaging increase EAC resistance include:

- the promotion of homogeneous deformation which may limit hydrogen transport along planar slip bands and lower grain boundary stresses [23, 24, 26, 28, 45]

- the increase of the electrochemical nobility of the η' precipitates and the prevention of hydrogen uptake by limiting dissolution of grain boundary precipitates [44, 45, 53, 54]

- the increase of the hydronium ion reduction rate and the subsequent hydrogen recombination at copper rich particles, which may:
  - consume hydronium ions and limit acidification in occluded geometries [55] and
  - act as beneficial trap states, preventing hydrogen from interacting with the crack tip process zone. Note that in-situ TEM experiments have reported gas bubbles (presumably H_2) formed at unidentified copper rich grain boundary particles in 7XXX series alloys when exposed to humid air [4, 56-58].

- in Al-Cu binary alloys, copper increases the apparent hydrogen solubility although its effect in multicomponent alloys is not well understood [59]. At a fixed concentration in a closed system, increased hydrogen solubility (from either increased interstitial solubility or the effect of innocuous trap states) may limit the amount of hydrogen that migrates to high angle grain boundaries and promotes intergranular cracking.

Objectives of this Research

Hydrogen controlled EAC stage II crack growth rate data are lacking for 7XXX series alloys in the UA, PA, and OA tempers. The possible benefits of alloyed copper on HEAC resistance have never been examined in tests which de-couple hydrogen effects from aqueous dissolution. No crack growth rate data exist for AA 7050 in humid air and little work has been done to systematically assess the effects of aging and copper level on crack growth kinetics under hydrogen embrittlement control. The present work seeks to investigate the humid air cracking of a modern 7XXX series alloy (AA 7050) in 90% RH air as a function of temper, temperature, and alloyed copper level. Establishing the effects of these variables on the

hydrogen embrittlement controlled stage II crack growth rate will aid in the progress toward a mechanistic understanding of HEAC and to developing high strength, HEAC resistant tempers and alloys.

EXPERIMENTAL PROCEDURE

Materials and Microstructure

The AA 7050 and the low copper variant of AA 7050 were supplied by the Aluminum Company of America in final heat-treated form. The chemical composition of each material is given in Table 3. Zinc and magnesium are alloyed primarily for precipitation hardening. Copper decreases the solubility of Mg and Zn [29, 47] and additions > 1 wt.% are known to improve EAC resistance [43, 45]. Zirconium is added to form coherent Al_3Zr dispersoids which help control the grain size and improve quench sensitivity relative to incoherent Cr bearing dispersoids [29, 47].

The AA 7050 material was heat-treated from a commercially produced 6" thick plate. The low copper material was from a 2" thick plate produced at the Alcoa Technical Center. Samples were taken from the T/4 plane of the 6" AA 7050 plate and the T/2 plane of the 2" thick low copper material. The heat treatments used are summarized in Table 4. The precipitation sequence in AA 7050 is given in Equation 6 where η' is a metastable precipitate and η is the equilibrium phase ($MgZn_2$) [29, 30, 60, 61].

$$\textit{Supersaturated Solid Solution} \rightarrow \textit{G.P. Zones} \rightarrow \eta' \rightarrow \eta \qquad (6)$$

Additionally, the constituent *S* phase (Al_2CuMg) may be present in the alloy [51, 60, 62]. The *S* phase precipitates in Al-Mg-Cu alloys in a process similar to Equation 6 and is thought to form between 450 and 500 °C [51, 63, 64]. The stable *T* phase does not form in 7050-type alloys because the Mg/Zn ratio is < 1 [48, 61]. Constituent particles in AA 7050 include Al_7Cu_2Fe, Mg_2Si, and Al_2CuMg [48, 65].

Selected mechanical and physical properties of each of the materials are given in Table 5. The microstructure of AA 7050 and the low copper variant are shown in Figure 1. Typical dimensions of the pancake shaped, unrecrystallized grains are approximately 1000 μm (L) x 250 μm (T) x 75 μm (S). The unrecrystallized grains in Figure 1 contain a pronounced dislocation substructure that is attacked by Keller's reagent while recrystallized grains remain bright. Note the similar grain structure and degree of recrystallization for the AA 7050 and the low copper material. Mechanical testing in a separate program revealed the peak strength of the low copper alloy to be ~9% higher than the strength of the "peak aged" material in the present study [66]. Therefore, it is important to note that *the peak aged thermal treatment actually produced a slightly overaged microstructure in the low copper alloy.* However, to facilitate the discussion, the term "peak aged" will be used to describe both the AA 7050 and the low copper alloy that was processed at the 154 °C, 12 hour thermal treatment.

Crack Growth Rate Testing

Crack growth rate experiments in 90% RH air were conducted on double-cantilever beam (DCB) fracture mechanics specimens held at constant crack mouth opening displacement (CMOD) by stainless steel bolts. The DCB specimens were machined in the S-L orientation from

the T/4 plane in the copper bearing 6" thick plate and the T/2 plane of the low copper 2" thick plate. Tests were conducted in 90% relative humidity air at temperatures of 25, 40, 60, and 90 °C. Precracks were introduced via mechanical overload in laboratory air, immediately prior to test initiation in humid air. Stress intensities were determined via compliance as outlined in a proposed ASTM standard by Committee G01 on Corrosion of Metals [67, 68].

After testing was completed, initial and final crack lengths were determined, from the average of five visual measurements taken across the width of the DCB specimens. These measurements were used instead of crack length measurements taken on the side of the DCB specimen since tunneling of the crack adjacent to the sidewall was often observed. Additionally, internally strain gauged bolts were utilized in the 25 °C test to provide a record of load vs. exposure time and confirm K independence of the crack growth rate data (Figure 2). Replicate tests over different ΔK ranges were performed at 90 °C for selected tempers in order to confirm the K independence of the stage II crack growth rates at elevated temperature (Figure 3).

RESULTS

Effect of Temper on Crack Growth Rate

All tempers of AA 7050 and the low copper variant underwent crack growth when exposed to 90% relative humidity air. The stage II crack growth rate data for each material and temper are summarized in Figures 3 and 4. At 25, 40, and 60 °C the crack growth rate from fastest to slowest is: 7050 UA > low Cu PA > low Cu OA > 7050 PA > 7050 OA. At 90 °C the order of low Cu OA and 7050 PA are reversed. These trends are in general agreement with what is known about aqueous EAC resistance in Al-Zn-Mg alloys: *i.e.*, crack growth rate decreases as

the material is heat treated from underaged to peak aged and stage II crack growth rates are relatively K independent [2, 17, 41, 45, 52, 69]. Moreover, low copper alloys crack faster than higher copper (> 1 wt.%) Al-Zn-Mg alloys as seen elsewhere [41, 45]. The combined effects of temper and test temperature are shown in Figure 4. Note the strong dependence of crack growth rate on test temperature for each alloy and temper.

For both AA 7050 and the low copper alloy, a benefit of overaging on the crack growth rate in 90% RH air is observed at all temperatures as shown in Figure 4. However, the higher copper AA 7050 shows a significantly greater benefit of overaging (~ 10 times lower CGR at 25 °C relative to peak aged AA 7050) than the low copper material (~2.5 times lower CGR at 25 °C relative to the peak aged low copper alloy), consistent with the observations of Sarkar and Starke tested in aqueous solution (i.e. drop-wise addition of 3.5 wt.% NaCl) [45]. The maximum differences between AA 7050 UA, PA, and OA tempers occurred at room temperature and the minimum differences at 90 °C. A similar effect is seen for the difference in crack growth rate between the high and low copper alloys.

Effect of Alloyed Copper

Note that comparisons between the AA 7050 and the low copper Al-Zn-Mg alloy are difficult since the intended "peak aged" thermal treatment used for both the commercial alloy and the low copper variant actually produces a slightly overaged microstructure in the low copper alloy. Figure 5 compares the crack growth rates of the normal copper and low copper alloys relative to their degree of overaging. In this analysis, peak strength was taken as 532 MPa for the AA 7050 copper bearing alloy and 477 MPa for the low copper alloy [66]. Once the data

are normalized to peak strength, it can be seen from Figure 5 that at equivalent degrees of overaging, the trend is toward reduced crack growth rates in the high copper, commercial AA 7050 relative to the low copper alloy.

Activation Energy Analysis

Hyatt and Speidel showed that the stage II crack growth rate of AA 7079-T651 exposed to 3M KI solution held at –700 mV vs. a saturated calomel electrode was a thermally activated process, well fitted by an Arrhenius-type equation (Equation 7) where v_{II} is the stage II crack growth rate, v_0 is a constant, $Q_{Effective}$ is the effective activation energy for stage II crack growth, R the gas constant and T the temperature [1, 2]. This Arrhenius-type temperature dependence also describes the stage II crack growth rates observed in the HEAC environment of the present study as shown by the linearity of the data in Figure 6. The slope of the lines in Figure 6 is proportional to the activation energy for cracking, $Q_{Effective}$, and the y-intercept is equal to the pre-exponential, v_0 as given by Equation 7. These data are summarized in Table 6 and shown graphically in Figure 7. Note that in copper bearing AA 7050, both $Q_{Effective}$ and v_0 increase with increasing aging time. Increases in $Q_{Effective}$ produce slower crack growth rates while increases in v_0 produce higher crack growth rates. Additionally, both $Q_{Effective}$ and v_0 are significantly lower in the low copper alloy relative to AA 7050.

$$v_{II} = v_0 \, exp\left(-Q_{Effective}/RT\right) \qquad (7)$$

Stage II HEAC Fracture Path

Metallographic cross sectioning of stage II HEAC cracks (Figure 8) reveals a predominately intergranular path of the HEAC cracks in all tempers. Moreover, intergranular cracking was seen at all test temperatures (25-90 °C). For all alloys and tempers, test temperature did not appear to alter the fracture path from the high angle grain boundaries. The fracture surfaces are relatively flat with small facets corresponding to subgrain dimensions. Additionally, cross sections revealed that secondary cracking was of limited depth, usually extending less than one grain deep, adjacent to the main crack (< 200 microns) and in all cases < 500 microns from the main crack.

A typical transition between the HEAC and fast fracture regions is shown in Figure 9. For all tempers, there is a distinct transition between the faceted, intergranular fracture mode of the HEAC region and the more ductile fast fracture region where microvoids are commonly observed. The HEAC regions from each material are compared in Figure 10. Note the flat, faceted fracture surface, typical of cracking along the face of a pancake shaped grain (Figure 1) was common to all materials. In the AA 7050 material (Figure 10 a, b, and c) 1-3 micron diameter particles are seen on the fracture surface. Energy dispersive x-ray analysis showed that these particles are rich in Al, Zn, and Cu indicating that they are *S* phase (Al_2CuMg) constituent particles. No *S* phase particles were observed in the low copper alloy. Additionally, a replicate test on AA 7050-OA with and without *S* phase particles showed no significant difference (1.26×10^{-10} m/s with *S* vs. 1.25×10^{-10} m/s without *S* at 25 °C) in crack growth rate suggesting that the presence of *S* phase particles has limited effect on HEAC crack growth rate tests conducted in humid air.

Fractography of mating fracture surfaces (Figure 11) of the fastest cracking (AA 7050-UA) and the slowest cracking (AA 7050-OA) tempers tested at 90 °C and 90% RH showed very good correspondence to each other. Matching features on the order of 100 nm (0.1 μm) can be resolved indicating that very little corrosion has occurred [70]. High magnification of HEAC fracture surfaces shows rows of closely spaced (~0.5 μm), parallel marking (Figure 12) which suggest that crack advance occurs in discontinuously.

DISCUSSION

The Effect of Copper on HEAC

As shown in Figures 3-5 it is clear that even though the "peak aged" low copper alloy is actually slightly overaged, it still cracks faster at each temperature than the truly peak aged AA 7050. In fact, the low copper alloy would have to be aged beyond the OA temper utilized in the present study in order to achieve the lower stage II crack growth rate of the PA copper bearing material. Therefore, it appears that copper plays a critical role in both aqueous and hydrogen environment assisted cracking. As discussed in the Background, copper or copper bearing precipitates may :

1. Promote homogeneous slip
2. Limit electrochemical dissolution of grain boundary precipitates
3. a) Promote H recombination and

   b) prevent acidification by facilitating the reduction of H^+ ions local to the crack tip
4. Act to create a specific, beneficial H trap state
5. Influence H solubility and diffusivity

The work of Starke *et al.* has shown that copper additions > 1 wt.% promote homogenous deformation and likely play a significant role in EAC resistance [26, 27, 45]. In the present study, crack growth rate testing was conducted in a HEAC controlled environment, where water was unlikely to be condensed at the crack tip. Therefore, effects 2 and 3b are disregarded. In-situ TEM experiments of Christodoulou indicate that copper rich particles may act as beneficial trap states (effect 4) [11, 57]. Additionally, alloyed copper or copper bearing particles may increase hydrogen solubility (effect 5) [59, 71, 72]. For a fixed hydrogen concentration in a closed system, increased lattice solubility may decrease the amount of hydrogen that segregates to internal interfaces (*e.g.*, grain boundaries) and promotes cracking. Similarly, strong hydrogen traps may increase the apparent solubility and prevent or delay hydrogen from interacting with the crack tip process zone.

Role of Creep in HEAC

Since the stage II crack growth rate tests were conducted at homologous temperatures between ~0.40-0.48, an additional consideration is that creep may contribute to the observed crack growth rates. Little data is available for the creep crack growth rates in AA 7050 although the study of Sarioglu *et al.*, on AA 7050-T73651 suggests that creep rates may be small relative to the HEAC stage II crack growth rates observed in the present study [73]. These authors found creep crack growth rates in the L-S orientation at 150 °C in laboratory air were ~ 10^{-7} mm/s at a stress intensity of 30 MPa$\sqrt{m}$ which is ~ 3 orders of magnitude lower than the stage II crack growth rate observed at 90 °C (S-L orientation).

While creep rates may be faster in the S-L orientation, the lower temperatures used in the crack growth rate tests should act to offset any effect of specimen orientation. If the creep crack growth rate is governed by dislocation creep between 25 and 90 °C, then the difference between creep crack growth rates between 150 and 90 °C is proportional to the self-diffusivity of aluminum over the temperature [74]. For self-diffusion of aluminum, a change in temperature from 150 to 90 °C, lowers the self-diffusivity over 100 times [75]. These results indicate that creep crack growth should have a negligible contribution to the HEAC stage II crack growth rates.

Additional support for a negligible contribution of creep crack growth comes from the aqueous EAC tests of L.M. Young and R.P. Gangloff [17, 76]. These researchers saw little evidence of creep crack growth in EAC resistant tempers of AA 7050 at 25 °C suggesting that creep crack growth rates are $< 10^{-7}$ mm/s. Similarly, the HEAC crack growth rate data of Hyatt and Speidel [1,2] indicate that environmental effects dominate crack growth rate and that any creep contribution is $\leq 5 \times 10^{-8}$ mm/s at 21 °C.

Analysis of v_0 and $Q_{Effective}$

Analysis of stage II crack growth rate data in both humid air and aqueous solutions shows that an Arrhenius-type equation accurately describes the observed crack growth rates over the temperature ranges investigated (25-90 °C). Therefore, it is important to understand which physical processes may affect v_0 and $Q_{Effective}$ (*e.g.*, hydrogen production, adsorption, diffusion, trapping, etc.). Once the physical processes that comprise v_0 and $Q_{Effective}$ are established, it may be possible to alter the chemistry or the processing of the alloy to improve EAC resistance.

While no direct comparisons to the HEAC cracking data of AA 7050 are available, some general comparisons can be made. The data of Lee [77] shows that both the activation energy for cracking, $Q_{Effective}$, and the pre-exponential, v_0, increase with the degree of overaging, which is consistent with the observations of this study. These observations indicate that overaging alters thermally activated processes which are part of the EAC mechanism.

Recent research into the diffusivity of hydrogen indicates that in AA 7050, there is excellent correlation between the change in the apparent activation energy for hydrogen diffusion and crack growth in humid air as the alloy is aged from the peak aged to the overaged temper (Table 7) [14]. In the copper bearing alloy, overaging increases the apparent activation energy for stage II crack growth and for hydrogen diffusion by approximately 16 kJ/mol. In the low copper alloy, overaging produced no significant increase in the apparent activation energy for hydrogen diffusion or stage II crack growth within experimental error [14, 78]. These results suggest that the benefit of overaging a copper bearing alloy is to slow the hydrogen transport kinetics to the crack tip process zone.

It is important to note that while the *changes* in activation energy with overaging for crack growth in humid air and hydrogen diffusion are in good agreement, the actual activation energies for crack growth in humid air (~58-99 kJ/mol) are significantly greater than those observed for hydrogen diffusion (14-33 kJ/mol) [14]. It is likely that one or more thermally activated processes such as hydrogen production (~28-47 kJ/mol) and hydrogen entry (~39-97 kJ/mol) contribute to crack growth (Table 8).

Unfortunately, not enough is known about fundamental parameters such as the activation energy for hydrogen adsorption, the heat of solution of hydrogen, and the activation energy for hydrogen production via humid air oxidation to quantitatively assess the cracking process in AA 7050. However, it is informative to qualitatively compare HEAC crack growth rate models with the criteria listed in Table 9 and with heuristic observations of the effects of temper and alloyed copper.

Comparison of Experimental and Heuristic Observations

The observation that EAC of Al-Zn-Mg alloys requires the presence of water is consistent with a HEAC mechanism where large hydrogen fugacities can be produced by small amounts of water via the oxidation of aluminum. The *K*-independent regime of crack growth suggests that crack advance is not limited by mechanical damage but by other processes such as hydrogen production or transport to the process zone. The large range in apparent activation energies for crack growth (16-118 kJ/mol in the literature and 58-99 kJ/mol in this study) appear to be bounded at the lower extreme by the apparent activation energy for hydrogen diffusion [14, 78].

The strong effects of temper and copper on the stage II crack growth rate are related to the processes which govern the pre-exponential, v_0, and activation energy, $Q_{Effective}$, for crack growth. The empirical observation that copper additions are beneficial to EAC is traceable to its effect on the apparent activation energy for crack growth. This increase in $Q_{Effective}$ for crack growth is

likely related to copper's ability to increase the apparent activation energy for hydrogen diffusion in the overaged temper [14, 78].

CONCLUSIONS

- Cracking of AA 7050 and a low copper variant in 90% RH air over the temperature range 25-90 °C is controlled by hydrogen environment assisted cracking, which is consistent with previous studies on other 7XXX series alloys [1, 2].

- For each alloy and temper studied, the stage II crack growth rate in 90% RH air increased with increasing temperature over the range 25-90 °C and can be accurately described by an Arrhenius-type equation.

- For identical thermal aging treatments, the low copper alloy cracked faster in stage II than copper bearing AA 7050 between 25 and 90 °C, confirming the beneficial effect of copper on HEAC resistance.

- The resistance to hydrogen environment assisted cracking (*i.e.*, the stage II crack growth rate) of AA 7050 follows the empirically known trend for aqueous EAC; EAC resistance increases as a 7XXX alloy is tempered from underaged to overaged.

- In the low copper alloy, overaging has a limited effect because the activation energy for crack growth is not changed. Rather, the pre-exponential (v_0) is decreased which results in a modest change in crack growth rate as compared to copper bearing alloys.

- In the copper bearing alloy, the large decrease in crack growth rate in the overaged temper is attributed to a significant (~16 kJ/mol) increase in the apparent activation energy for stage II crack growth relative to the peak aged temper. This increase in activation energy for crack growth corresponds well with that for the apparent activation energy for hydrogen diffusion.

- In all tempers, at test temperatures between 25 and 90 °C, the HEAC fracture path was intergranular, predominantly along high angle grain boundaries.

- The observation of a finite stage II crack growth rate in AA 7050-OA shows that this temper is not intrinsically immune to HEAC. Instead, the apparent activation energy for some kinetic factors such as hydrogen diffusion are altered such that the observed crack growth rates are significantly slower than in underaged or peak aged AA 7050.

ACKNOWLEDGEMENTS

The authors wish to thank E. Colvin, J. Moran, G. Nitowski, J.T. Staley, P. Vandenburgh, and H. Weiland, of the Alcoa Technical Center for their technical and financial support. R.P. Gangloff

and L.M. Young of the University of Virginia provided valuable experimental advice and critical review of the manuscript. Additional financial support was graciously given by the National Science Foundation (DMR-9357463) and by Mobil MEPTEC.

REFERENCES

1. Hyatt, M.V. and M.O. Speidel, *Stress-Corrosion Cracking of High-Strength Aluminum Alloys*, Report No. D6-24840, Boeing, Seattle, WA, 1970.
2. Speidel, M.O., *Hydrogen Embrittlement and Stress Corrosion Cracking of Aluminum Alloys*, in Hydrogen Embrittlement and Stress Corrosion Cracking, Gibala and Hehemann, editors, ASM, p. 271-296, 1984.
3. Watkinson, F.E. and J.C. Scully, "The Effect of Atmospheric Moisture Upon the S.C.C. of an Al-6Zn-3Mg Alloy", *Corrosion Science*, Vol. 11, p. 179-182, 1971.
4. Christodoulou, L. and H.M. Flower, "Hydrogen Embrittlement and Trapping in Al-6%-Zn-3%-Mg", *Acta metall.*, Vol. 28, p. 481-487, 1980.
5. Tuck, C.D.S., "The Embrittlement of Al-Zn-Mg and Al-Mg Alloys by Water Vapor", *Met. Trans. A*, Vol. 16A, p. 1503-1514, 1985.
6. Scamans, G.M., R. Alani, and P.R. Swann, "Pre-exposure Embrittlement and Stress Corrosion Failure in Al-Zn-Mg Alloys", *Corrosion Science*, Vol. 16, p. 443-459, 1976.
7. Scamans, G.M., "Stress Corrosion Cracking of Aluminium Alloys by Hydrogen Embrittlement", *Aluminium*, Vol. 58, p. 332-334, 1982.
8. Koch, G.H., "Hydrogen Induced Fracture of a High Strength Aluminum Alloy", *Corrosion*, Vol. 35, p. 73-78, 1979.
9. Vennett, R.M., *Trans. ASM*, Vol. 62, p. 1007, 1969.
10. Wei, R.P., *Rate Controlling Processes and Crack Growth Response*, in Hydrogen Effects in Metals, I.M. Bernstien and A.W. Thompson, editors, TMS-AIME, Moran, Wyoming, p. 677, 1980.
11. Christodoulou, L., *The Role of Hydrogen in the Environmental Failure of High Strength Aluminium Alloys*, Ph.D., Imperial College of Science and Technology, London, 1980.
12. Ricker, R.E. and D.J. Duquette, "The Role of Hydrogen in Corrosion Fatigue of High Purity Al-Zn-Mg Exposed to Water Vapor", *Met. Trans. A*, Vol. 19A, p. 1775-1783, 1988.
13. Lide, D.R., ed. CRC Handbook of Chemistry and Physics. 1991, CRC Press.
14. Young, G.A., *Hydrogen Environment Assisted Cracking of an Al-Zn-Mg-(Cu) Alloy*, Ph.D., University of Virginia, Charlottesville, 1999.
15. Do, T., S.J. Splinter, C. Chen, and N.S. McIntyre, "The Oxidation Kinetics of Mg and Al Surfaces Studied by AES and XPS", *Surf. Sci.*, Vol. 397(1-3), p. 192-198, 1997.
16. Uhlig, H.H., Corrosion and Corrosion Control. 3rd ed., John Wiley & Sons, New York, 1985.
17. Young, L.M., G.A. Young, J.R. Scully, and R.P.Gangloff. *The Effects of Electrode Potential and Temper on Environment Assisted Cracking in AA 7050* in *Lightweight Alloys for Aerospace Applications IV*. 1997. Orlando, FL, TMS.
18. Lewis, G.L., Thermodynamics, McGraw-Hill, 90-114, 1961.
19. Shih, C.F., "Relationship Between the J-Integral and the Crack Opening Displacement for Stationary and Extending Cracks", *J. Mech. Phys. Sol.*, Vol. 29(4), p. 305-326, 1981.
20. Marcus, P. and J. Oudar, eds., Corrosion Mechanisms in Theory and Practice. Corrosion Technology, ed. P.A. Schweitzer. 1995, Marcel Dekker, Inc., New York.
21. Albrecht, J., A.W. Thompson, and I.M. Bernstein, "The Role of Microstructure in Hydrogen Assisted Fracture of 7075 Aluminium", *Met. Trans. A*, Vol. 10A, p. 1759-1766, 1979.
22. Albrecht, J., I.M. Bernstein, and A.W. Thompson, "Evidence for Dislocation Transport of Hydrogen in Aluminium", *Met. Trans. A*, Vol. 13A, p. 811-820, 1982.

23. Hardwick, D.A., A.W. Thompson, and I.M. Bernstein, "The Effect of Copper Content and Microstructure on the Hydrogen Embrittlement of Al-6Zn-Mg", *Met. Trans. A*, Vol. 14A, p. 2517-2526, 1983.
24. Hardwick, D.A., A.W. Thompson, and I.M. Bernstein, "The Effect of Copper Content and Heat Treatment on the Hydrogen Embrittlement of 7050-Type Alloys", *Corrosion Science*, Vol. 28(12), p. 1127-1137, 1988.
25. Guyot, P. and L. Cottignies, "Precipitation Kinetics, Mechanical Strength and Electrical Conductivity of AlZnMgCu Alloys", *Acta Mater.*, Vol. 44(10), p. 4161-4167, 1996.
26. Lin, F.S. and E.A. Starke, "The Effect of Copper Content and Degree of Recrystallization on the Fatigue Resistance of 7XXX Type Aluminum Alloys I. Low Cycle Corrosion Fatigue", *Materials Science & Engineering*, Vol. 39, p. 27-41, 1979.
27. Lin, F.S. and J. E.A. Starke, "The Effect of Copper Content and Degree of Recrystallization on the Fatigue Resistance of 7XXX-Type Aluminum Alloys II. Fatigue Crack Propagation", *Materials Science & Engineering*, Vol. 43, p. 65-76, 1980.
28. Sanders, T.H. and E.A. Starke, "The Relationship of Microstructure to Monotonic and Cyclic Straining of Two Age Hardening Aluminum Alloys", *Met. Trans. A*, Vol. 7A, p. 1407-1417, 1976.
29. Staley, J.T., "Aging Kinetics of Aluminum Alloy 7050", *Met. Trans.*, Vol. 5, p. 929-932, 1974.
30. Bigot, A., *et al.*, "Tomographic Atom Probe Study of Age Hardening Precipitation in Industrial AlZnMgCu (7050) Alloy", *Materials Science Forum*, Vol. 217-222, p. 695-700, 1996.
31. Rao, B.V.N., "Influence of Aging Treatment on the Grain Boundary Precipitation and Chemistry in 7075 Al Alloy", *Met. Trans. A*, Vol. 12A, p. 1356-1359, 1981.
32. Rajan, K., W. Wallace, and J.C. Beddoes, "Microstructural Study of a High-Strength Stress-Corrosion Resistant 7075 Aluminum Alloy", *J. Materials Science*, Vol. 17, p. 2817-2824, 1982.
33. Scamans, G.M., N.J.H. Holroyd, and C.D.S. Tuck, "The Role of Magnesium Segregation in the Intergranular Stress Corrosion Cracking of Aluminium Alloys", *Corrosion Science*, Vol. 47(4), p. 329-347, 1987.
34. Pickens, J.R., T.J. Langan, and J.A.S. Green, *Mechanisms of Stress-Corrosion Cracking in Al-Zn-Mg and Al-Mg Alloys*, in Environment Sensitive Fracture of Metals and Alloys, United States Navy, Washington, D.C., 1987.
35. Hepples, W., M.R. Jarrett, J.S. Crompton, and N.J.H. Holroyd, *The Influence of Microstructure on the Stress Corrosion Cracking and Exfoliation of Commercial Al-Zn-Cu Alloys*, in Environment-Induced Cracking of Metals, R.P. Gangloff and M.B. Ives, editors, ASM/NACE/TMS, Kohler, Wisconsin, p. 383-387, 1988.
36. Chen, J.M., "Grain Boundary Segregation of an Al-Zn-Mg Ternary Alloy", *Met. Trans. A*, Vol. 8A, p. 1935-1940, 1977.
37. Shastry, C.R. and G. Judd, "An Electron Microprobe Analysis of Solute Segregation Near Grain Boundaries in an Al-Zn-Mg Alloy", *Met. Trans.*, Vol. 3, p. 779-782, 1972.
38. Montgrain and Swann, in Hydrogen Effects in Metals, I.M. Bernstein, editor, 1974.
39. Song, R.G., *et al.*, "Grain Boundary Segregation and Hydrogen-Induced Fracture in 7050 Aluminum Alloy", *Acta Mat.*, Vol. 44(8), p. 3241-3248, 1996.
40. Viswanadham, R.K., T.S. Sun, and J.A.S. Green, "Grain Boundary Segregation in Al-Zn-Mg Alloys-Implications to Stress Corrosion Cracking", *Met. Trans. A*, Vol. 11A, p. 85-89, 1980.
41. Holroyd, N.J.H., *Environment-Induced Cracking of High-Strength Aluminum Alloys*, in Environment-Induced Cracking of Metals, R.P. Gangloff and M.B. Ives, editors, ASM/NACE/TMS, Kohler, Wisconsin, p. 311-345, 1988.
42. Schmiedel, H. and W. Gruhl, "The Influence of the Zn-, Mg-, and Cu-Concentrations at the Grain boundaries on the Stress Corrosion Susceptibility of AlZnMg-Alloys", *Z. Metallkde*, Vol. 74, p. 777-782, 1983.
43. Staley, J.T., *History of Wrought Aluminum Alloy Development*, Report No. 56-86-AS1, Alcoa, 1986.
44. Staley, J.T., S.C. Byrne, E.L. Colvin, and K.P. Kinnear, "Corrosion and Stress-Corrosion of 7XXX-W Products", *Materials Science Forum*, Vol. 217-222, p. 1587-1592, 1996.
45. Sarkar, B., M. Marek, and E.A. Starke, "The Effect of Copper Content and Heat Treatment on the Stress Corrosion Characteristics of Al-6zn-2Mg-X Cu Alloys", *Met. Trans. A*, Vol. 12A, p. 1939-1943, 1981.
46. Starke, E.A., *Alloying Aluminum: Development of New Aluminum Alloys*, in Alloying, J.L.Walter, M.R. Jackson, and C.T. Sims, editors, ASM International, Metals Park, p. 165-197, 1988.
47. Starke, E.A., *Heat-Treatable Aluminum Alloys*, in Aluminum Alloys - Contemporary Research and Applications, A.K. Vasudevan and R.D. Doherty, editors, Academic Press, p. 35-63, 1989.

48. Hatch, J.E., Aluminum Properties and Physical Metallurgy, ASM, Metals Park, OH, 1984.
49. Chinh, N.Q., *et al.*, "Precipitation in Al-Zn-Mg-(Cu,Zr) Alloys", *Z. Metallkd.*, Vol. 88(8), p. 607-611, 1997.
50. Livak, R.J. and J.M. Papazian, "Effects of Copper on Precipitation and Quench Sensitivity of Al-Zn-Mg Alloys", *Scripta Met.*, Vol. 18, p. 483-488, 1984.
51. Fujikawa, S., T. Hara, A. Ishida, and K. Hirano, "A Calorimetric Study of Precipitation Process in Al-Zn-Mg-Cu Alloys", *Thermochimica Acta*, Vol. 85, p. 171-174, 1985.
52. Speidel, M.O., "Stress Corrosion Cracking of Aluminum Alloys", *Met. Trans. A*, Vol. 6A, p. 631-651, 1975.
53. Doig, P., P.E.J. Flewitt, and J.E.Edingtion, "The Stress Corrosion Susceptibility of 7075 Al-Zn-Mg-Cu Alloys Tempered from T6 to an Overaged T7X", *Corrosion*, Vol. 22(6), p. 217-221, 1977.
54. Busby, J., J.F. Cleave, and R.L. Cudd, "The Effect of Copper and Silver Additions on the Stress-Corrosion-Resistance of Commercial Weldable Wrought Al-Zn-Mg Alloys", *J. Inst. Metals*, Vol. 99, p. 41-49, 1971.
55. Langan, T.J., *et al.*, "Simulation of the Crack Tip Chemistry of Stress Corrosion Cracks in 7XXX Aluminum Powder Alloys", *Corrosion*, Vol. 44(3), p. 165-169, 1988.
56. Alani, R. and P.R. Swann, "Water Vapor Embrittlement and Hydrogen Bubble Formation in Al-Zn-Mg Alloys", *Br. Corr. Jour.*, Vol. 12(2), p. 80-85, 1975.
57. Christodoulou, L. and H.M. Flower, *In-Situ H.V.E.M. Observations of Hydrogen Embrittlement*, in Hydrogen Effects in Metals, I.M. Bernstein and A.W. Thompson, editors, TMS, p. 493-501, 1980.
58. Scamans, G.M., "Hydrogen Bubbles in Embrittled Al-Zn-Mg Alloys", *Journal of Materials Science*, Vol. 13, p. 27-36, 1978.
59. Anyalebechi, P.N., ed. Analysis and Thermodynamic Prediction of Hydrogen Solution in Solid and Liquid Multicomponent Aluminum Alloys. Light Metals 1998. 1998, TMS, 827-842.
60. Lorimer, G.W., *Precipitation in Aluminum Alloys*, in Precipitation Processes in Solids, K.C. Russell and H.I. Aaronson, editors, TMS-AIME, Niagara Falls, NY, p. 87-119, 1976.
61. Cziraki, A., B. Fogarassy, and I. Gerocs, *Solid State Reactions in Al-Zn-Mg-Cu Alloys*, in Light Materials for Transportation Systems, N.J. Kim, editor, TMS, Kyongju, Korea, p. 391-405, 1993.
62. Morris, A.J., R.F. Robey, P.D. Couch, and E. DelosRios, "A Comparison of the Damage Tolerance of 7010 T7451 and 7050 T7451", *Materials Science Forum*, Vol. 242, p. 181-186, 1997.
63. Warmuzek, M., "An Influence of the Mg Content on the Structural Composition of the Al-Zn-Cu-Mg Alloys", *Mat. Sci. for.*, Vol. 215-216, p. 243-250, 1996.
64. Strawbridge, D.J., W. Hume-Rothery, and A.T. Little, "The Constitution of Aluminium-Copper-Magnesium-Zinc Alloys at 460 °C", *J. Inst. Met.*, Vol. 74, p. 191-225, 1948.
65. Starke, E.A., "Aluminium Alloys of the '70's: Scientific Solutions to Engineering Problems", *Materials Science and Engineering*, Vol. 29, p. 99-115, 1977.
66. Colvin, E.L., *Personal Communication*, , 1997.
67. Kane, R.D., *Making and Using Precrack Double Beam Stress Corrosion Specimens*, Report , ASTM G01.06, Houston, 1998.
68. Domack, M.S., *Evaluation of K_{ISCC} and da/dt Measurements for Aluminum Alloys*, in Environmentally Assisted Cracking: Science & Engineering, ASTM STP 1049, W.B. Lisagor, T.W. Crooker, and B.N. Leis, editors, ASTM, Philadelphia, PA, p. 391-409, 1990.
69. Speidel, M.O., *Current Understanding of Stress Corrosion Crack Growth in Aluminum Alloys*, in Theory of Stress Corrosion Cracking in Alloys, J.C. Scully, editor, NATO, Brussels, Belgium, p. 289-344, 1971.
70. Scamans, G.M., "Evidence for Crack-Arrest Markings on Intergranular Stress Corrosion Fracture Surfaces in Al-Zn-Mg Alloys", *Met. Trans. A*, Vol. 11A, p. 846-850, 1980.
71. Anyalebechi, P.N., "Analysis of the Effects of Alloying Elements on Hydrogen Solubility in Liquid Aluminum Alloys", *Scripta Met.*, Vol. 33(8), p. 1209-1216, 1995.
72. Anyalebechi, P.N., "Attempt to Predict Hydrogen Solubility Limits in Liquid Multicomponent Aluminum Alloys", *Scripta Mat.*, Vol. 34(4), p. 513-517, 1996.
73. Sarioglu, F., P. Abachi, and M. Doruk, "Crack Growth Kinetics of 7050-T73651 Aluminium Alloy Under Constant Load at 150 °C", *J. Mat. Sci.*, Vol. 28, p. 1430-1434, 1993.
74. Dieter, G.E., Mechanical Metallurgy, McGraw-Hill, 751, 1986.
75. Shewmon, P., Diffusion in Solids, TMS, 246, 1989.
76. Young, L.M. and R.P. Gangloff, *Unpublished Research*, The University of Virginia, 1997.
77. Lee, S.M., S.I. Pyun, and Y.G. Chun, "A Critical Evaluation of the Stress-Corrosion Cracking Mechanism in High-Strength Aluminum Alloys", *Met. Trans. A*, Vol. 22A, p. 2407-2414, 1991.

78. Scully, J.R., G.A. Young, and S.W. Smith, eds., Hydrogen Solubility, Diffusion, and Trapping in High Purity Aluminum, Al-Li-Cu, and Al-Zn-Mg-Cu Alloys. 2000.

Table 1. *Parameters used to evaluate the Kelvin equation (Equation 4).*

T (K)	298	313	363
γ (J/m^3)	7.275×10^{-2}	6.960×10^{-2}	6.082×10^{-2}
ρ_l (kg/m^3)	9.9821×10^{2}	9.9222×10^{2}	9.6535×10^{2}
ρ_g (kg/m^3)	1.73×10^{-2}	5.12×10^{-2}	4.23×10^{-1}
r_c (m)	1.00×10^{-8}	9.21×10^{-9}	7.13×10^{-9}

Table 2. *Parameters used to evaluate the crack tip radius (Equation 5).*

	AA 7050-PA	AA 7050-OA
n	0.1	0.10
dn	~0.76	~0.76
σ_{YS} (MPa) (S-T)	530	457
σ_{UTS} (MPa) (S-T)	596	533
σ_{Flow} (MPa)	563	495
σ_{UTS}/E	8.39	7.50
σ_{FLOW}/E	7.39	6.97

Table 3. *Chemical composition of the alloys used in this study (weight percent).*

Alloy	Zn	Mg	Cu	Zr	Si	Fe	Al	Mg/Zn
AA 7050 (spec.)	5.7-6.7	1.9-2.6	2.0-2.6	.08-.15	0.12	0.15	Bal.	0.28-0.45
AA 7050 (meas.)	6.09	2.14	2.19	0.11	0.05	0.09	Bal.	0.35
Low Cu 7050 (meas.)	6.87	2.65	0.06	0.10	0.04	0.10	Bal.	0.38

Table 4. *Temper designations and heat treatments.*

Temper	Heat Treatment
Underaged (UA)	467 °C / 2 hrs + Water Quench + 2% Stretch + 118 °C / 4 hrs
Peak Aged (PA)	7050-Underaged + 118 °C / 20 hrs + 154 °C / 12 hrs
Overaged (OA)	7050-Underaged + 163 °C / 27 hrs

Table 5. *Selected mechanical and physical properties. The symbol (L) refers to the longitudinal orientation and (ST) refers to the short transverse orientation. Note that the PA treatment is equivalent to the -T6 temper and the OA treatment equivalent to the -T74 temper.*

Alloy Temper	Yield Strength (MPa)	Tensile Strength (MPa)	% Elongation	Electrical Conductivity (%IACS)	Hardness Rockwell B
7050-UA	470 (L) 455 (ST)	533 (L) 554 (ST)	17 (L) 7 (ST)	30.8	90
7050-PA	538 (L) 532 (ST)	559 (L) 586 (ST)	12 (L) 4 (ST)	36.3	92
7050-OA	447 (L) 431 (ST)	508 (L) 509 (ST)	13 (L) 8 (ST)	41.5	86
Low Cu-PA*	476 (L) 432 (ST)	513 (L) 493 (ST)	14 (L) 7 (ST)	37.5	85
Low Cu-OA	388 (L) 349 (ST)	450 (L) 434 (ST)	16 (L) 11 (ST)	41.0	75

*Note that this microstructure is actually slightly overaged

Table 6. *Summary of the pre-exponential, v_0, and effective activation energy, $Q_{Effective}$, for crack growth in AA 7050 and a low copper variant tested in 90% RH air between 25 and 90 °C.*

Alloy Temper	Environment/ Temperature	v_0 (m/s)	95% Confidence Interval of v_0 (m/s)	$Q_{Effective}$ ± 95% Confidence (kJ/mol)
7050-UA	90% Relative Humidity Air 25-90°C	1.02×10^4	$0.31\text{-}3.38 \times 10^4$	66.4 ± 3.3
7050-PA		1.93×10^5	$0.52\text{-}7.09 \times 10^5$	82.1 ± 3.5
7050-OA		2.61×10^7	$0.92\text{-}7.43 \times 10^7$	98.4 ± 2.8
Low Cu-PA		1.92×10^2	$0.01\text{-}3.05 \times 10^3$	58.9 ± 7.4
Low Cu-OA		7.70×10^1	$0.11\text{-}5.45 \times 10^2$	58.8 ± 5.3

Table 7. *Comparison of the change in activation energy for stage II crack growth in humid air and the apparent activation energy for hydrogen diffusion [14].*

Alloy Temper	$Q_{Stage\ II}$ Crack Growth (kJ/mol)	Change in Q PA →OA (kJ/mol)	$Q_{Apparent}$ *Diffusivity of H* (kJ/mol)	Change in Q PA →OA (kJ/mol)
7050-PA	82.1	16.3	16.1	16.6
7050-OA	98.4		32.7	
Low Cu-PA	58.9	0.1	14.2	0.0
Low Cu-OA	58.8		14.2	

Table 8. *Comparison of the activation energies of some thermally activated processes that may be involved in hydrogen environment assisted cracking.*

Process	Alloy	Apparent Q (kJ/mol)	Reference
Corrosion rate in saturated water	1100	41.1	[79]
	5052	46.6	
	6061	28.5	
Hydrogen entry (heat of solution)	Al	39-97	[78]

Table 9. *Criteria to assess activated processes contributing to EAC.*

Empirical observations for EAC in 7XXX series alloys
• EAC does not occur in dry atmospheres, the presence of water is necessary
• A K-independent regime is usually observed although deviations have been reported
• Both temper and alloyed copper strongly affect stage II crack growth rates
• $Q_{Effective}$ ranges from 16-118 kJ/mol
• $Q_{Effective}$ appears to increase with aging time
• v_0 ranges from ~10^{-4}-10^{8} m/s
• The pre-exponential appears to increase with aging time and decrease with low copper levels

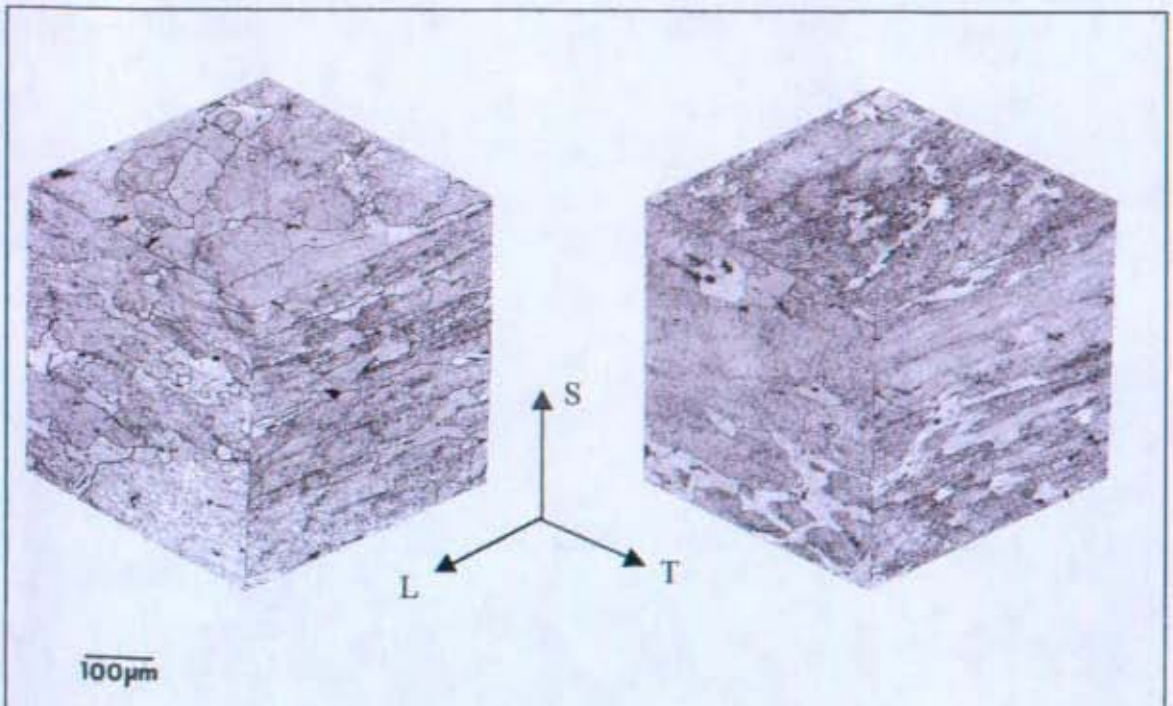

Figure 1. *Orthogonal metallographic views of the AA 7050 (left) and low copper material (right) showing the pancake shaped grain structure. Keller's reagent + Graff and Sargent's etch.*

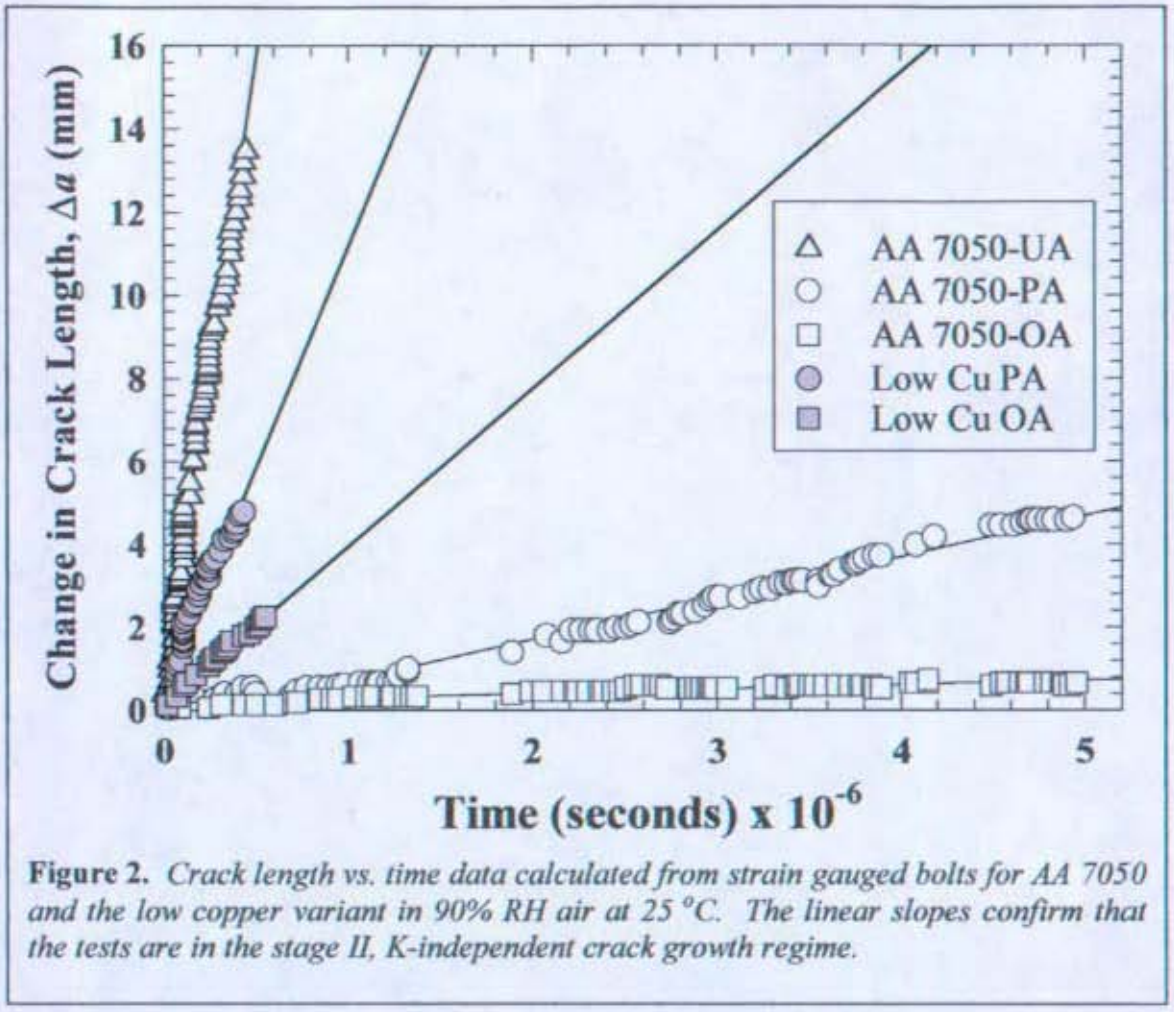

Figure 2. *Crack length vs. time data calculated from strain gauged bolts for AA 7050 and the low copper variant in 90% RH air at 25 °C. The linear slopes confirm that the tests are in the stage II, K-independent crack growth regime.*

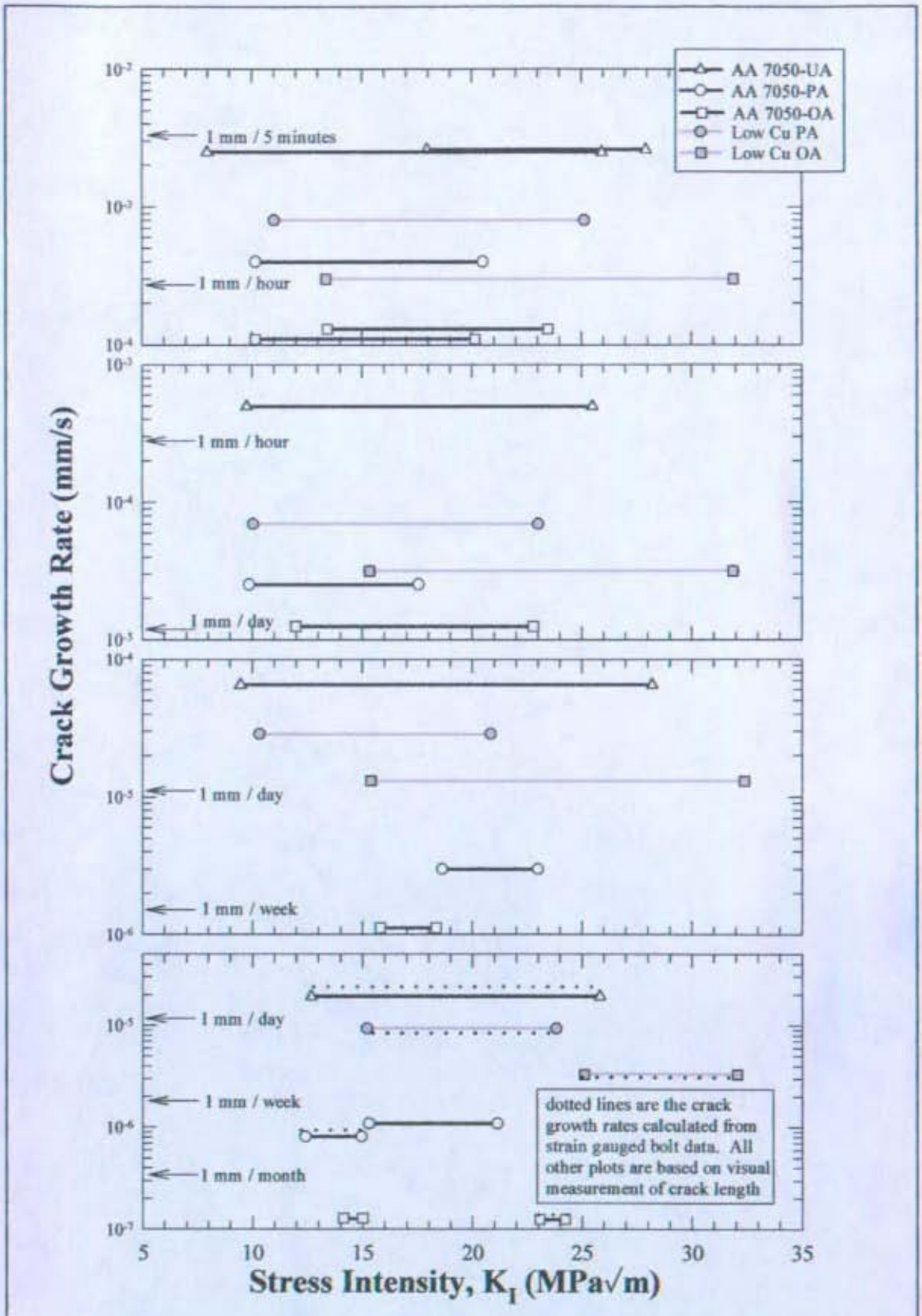

Figure 3. *Crack growth rate data in for AA 7050 and the low copper variant tested in 90% RH air as a function of temper and test temperature.*

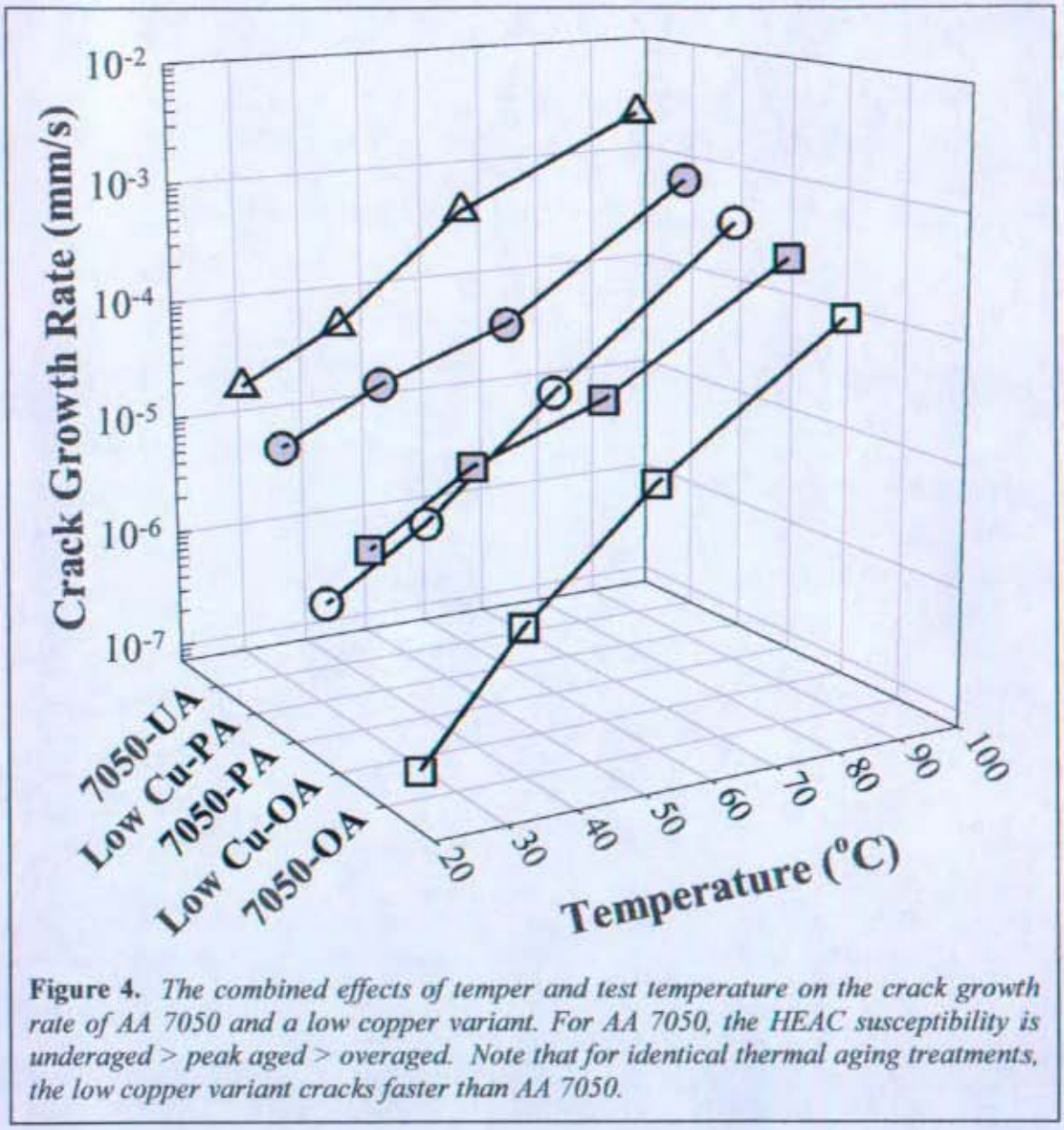

Figure 4. *The combined effects of temper and test temperature on the crack growth rate of AA 7050 and a low copper variant. For AA 7050, the HEAC susceptibility is underaged > peak aged > overaged. Note that for identical thermal aging treatments, the low copper variant cracks faster than AA 7050.*

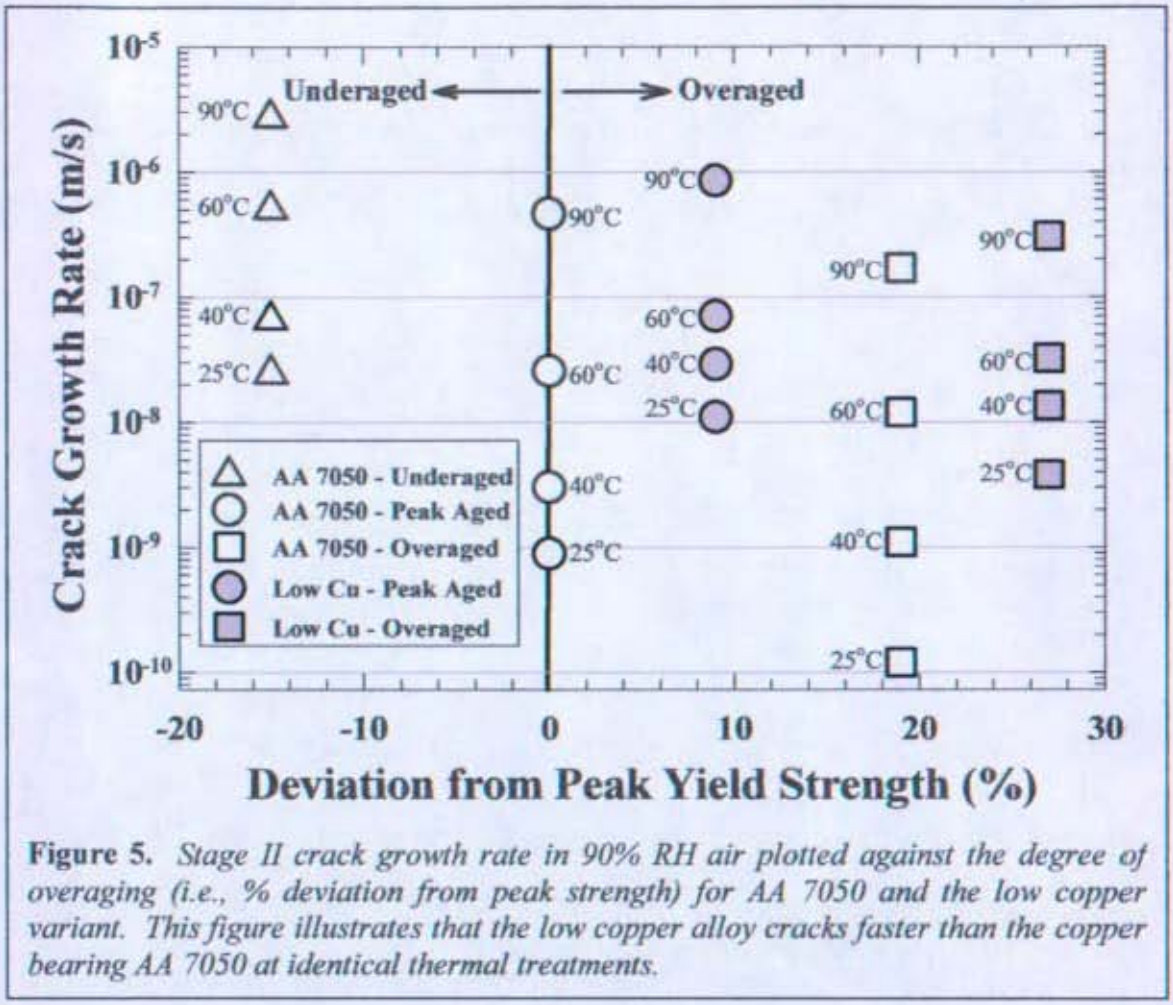

Figure 5. *Stage II crack growth rate in 90% RH air plotted against the degree of overaging (i.e., % deviation from peak strength) for AA 7050 and the low copper variant. This figure illustrates that the low copper alloy cracks faster than the copper bearing AA 7050 at identical thermal treatments.*

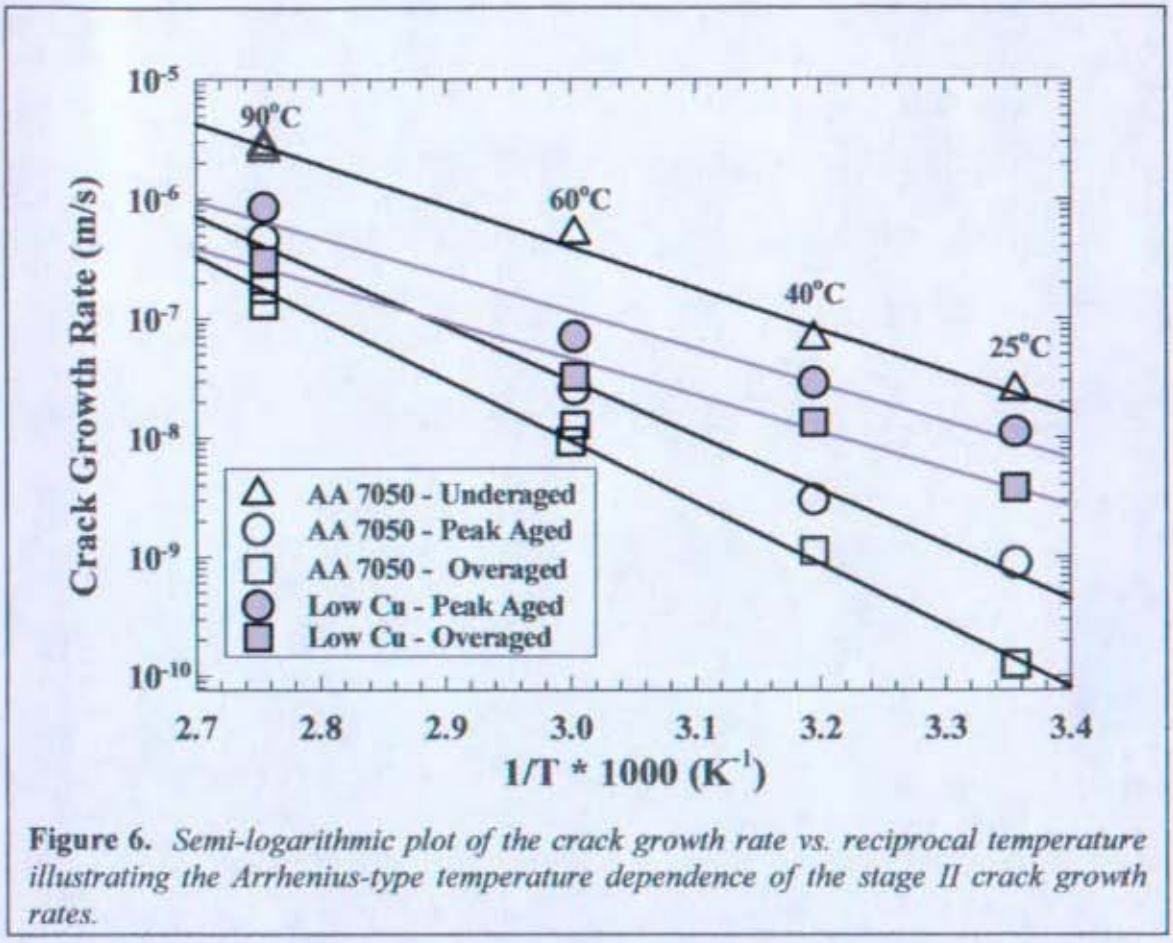

Figure 6. *Semi-logarithmic plot of the crack growth rate vs. reciprocal temperature illustrating the Arrhenius-type temperature dependence of the stage II crack growth rates.*

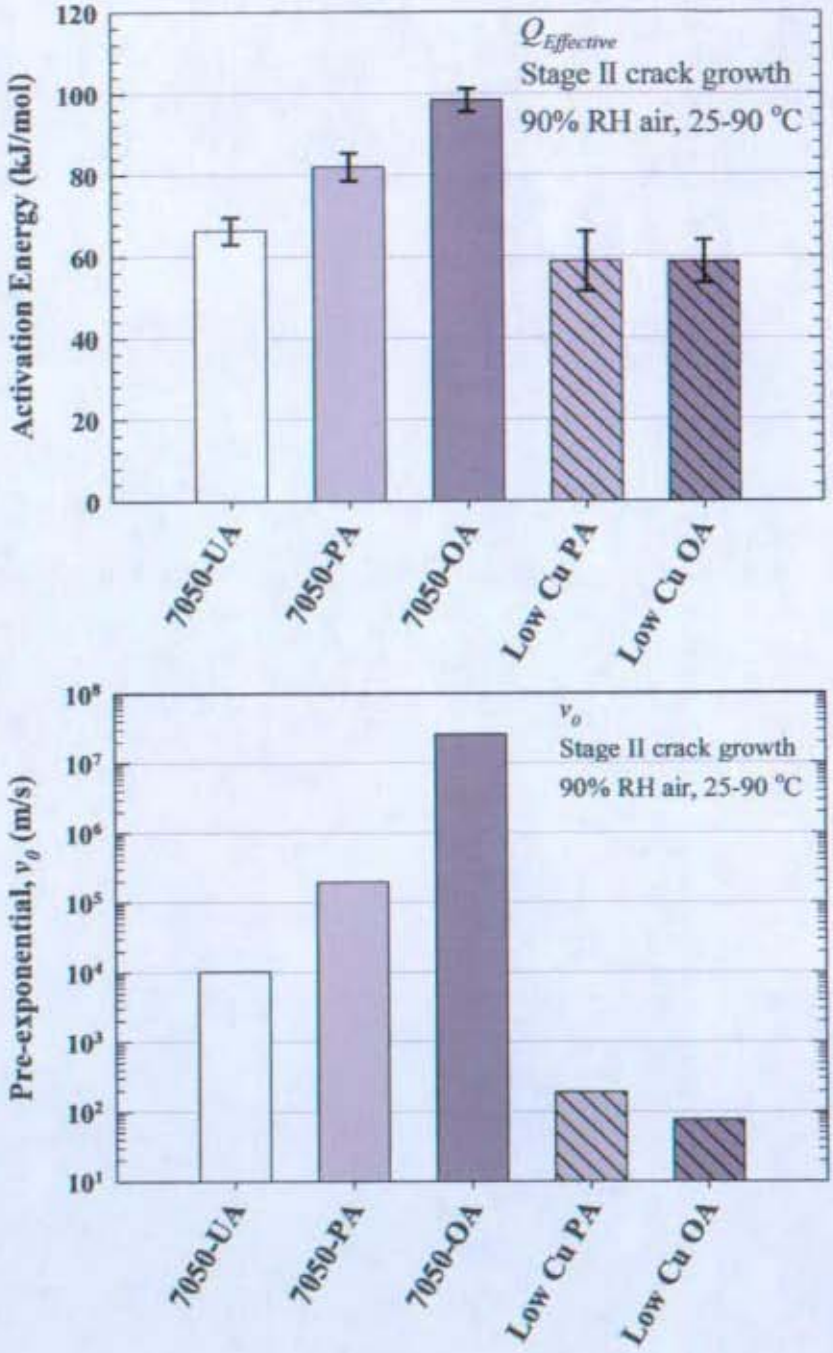

Figure 7. *Comparison of the activation energy, Q (top), and pre-exponential, v_0 (bottom) for stage II crack growth in 90% RH air.*

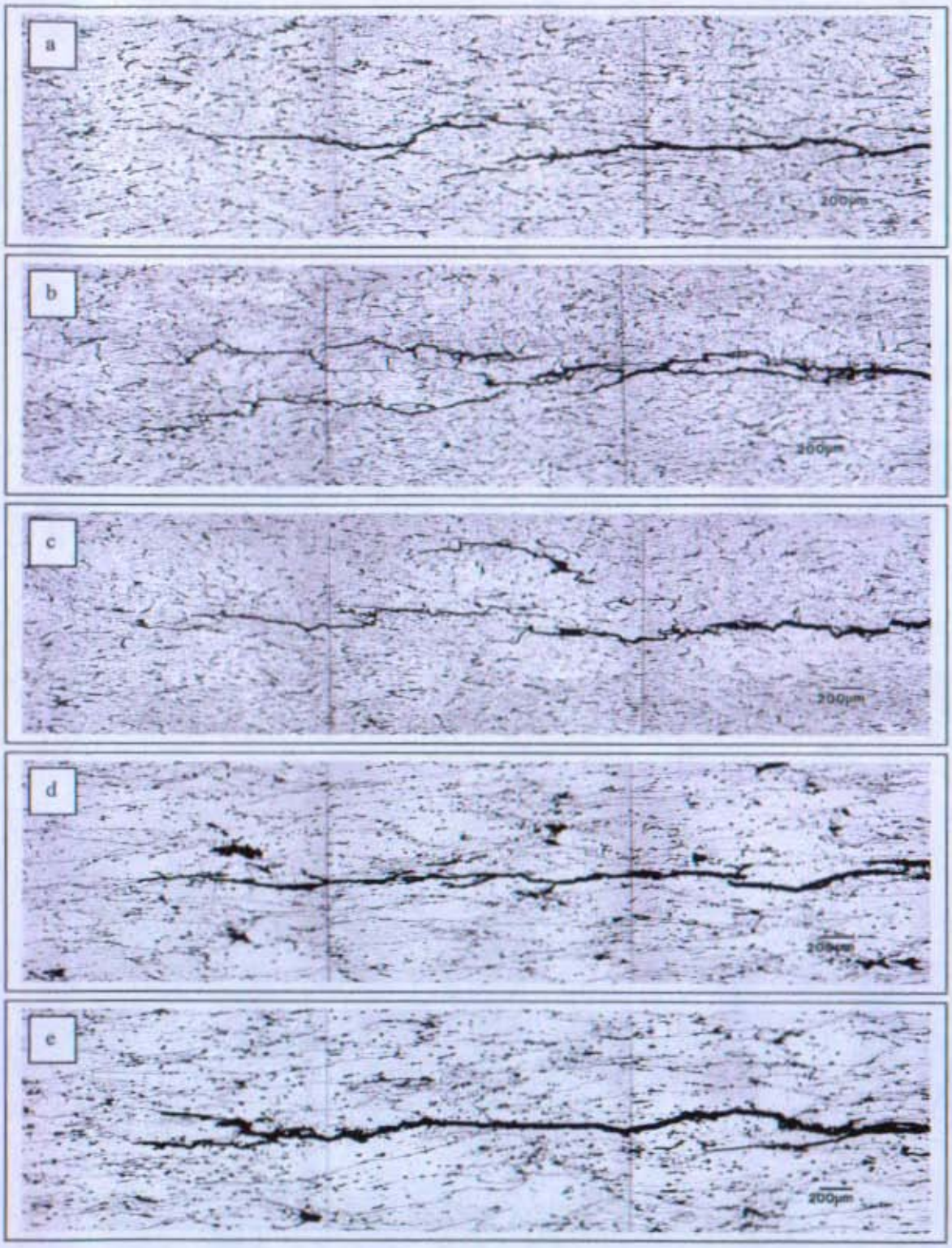

Figure 8. Metallographic cross sections from stage II HEAC cracks produced in 90 °C, 90% RH air illustrating the intergranular nature of the crack path a) 7050 UA, b) 7050 PA, c) 7050 OA, d) low Cu PA, and e) low Cu OA. Specimens were etched in 10% NaOH at 70 °C for 20 seconds, nitric acid rinse.

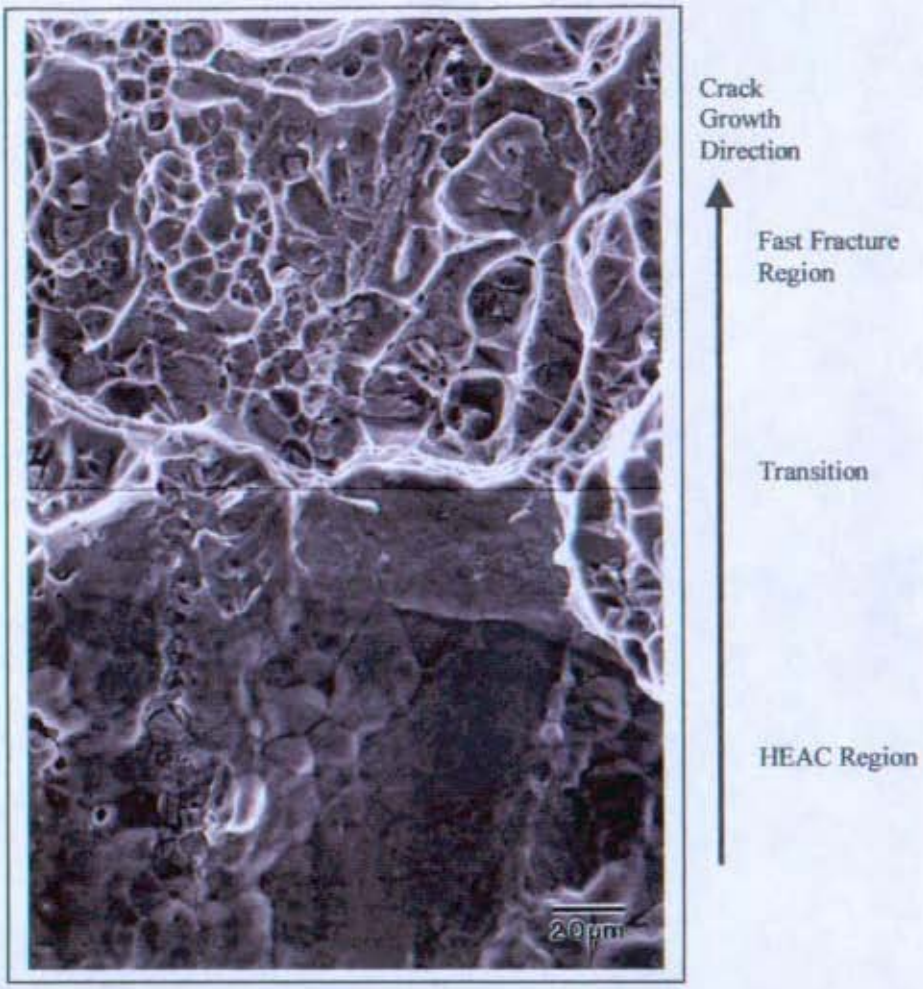

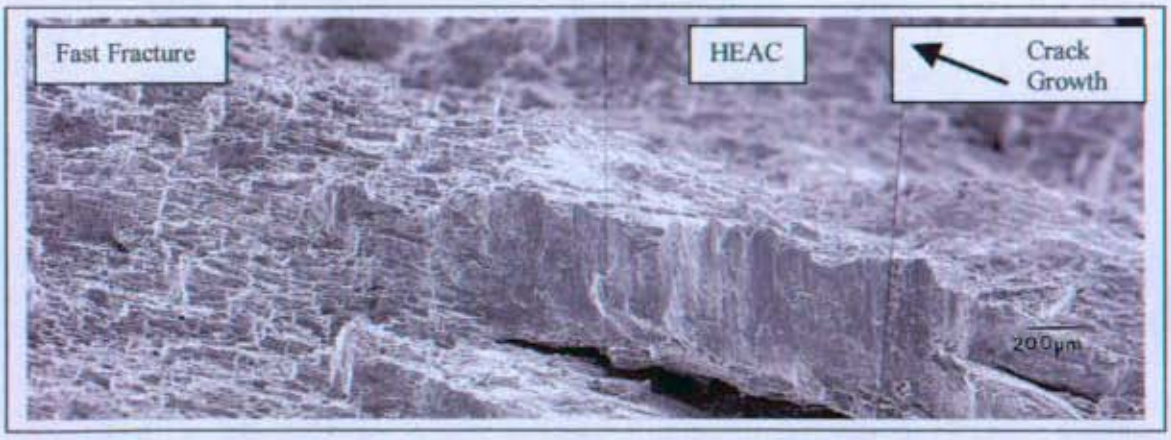

Figure 9. *Scanning electron micrographs of the HEAC/Fast Fracture transition in low copper–OA tested in 60 °C, 90% RH air.*

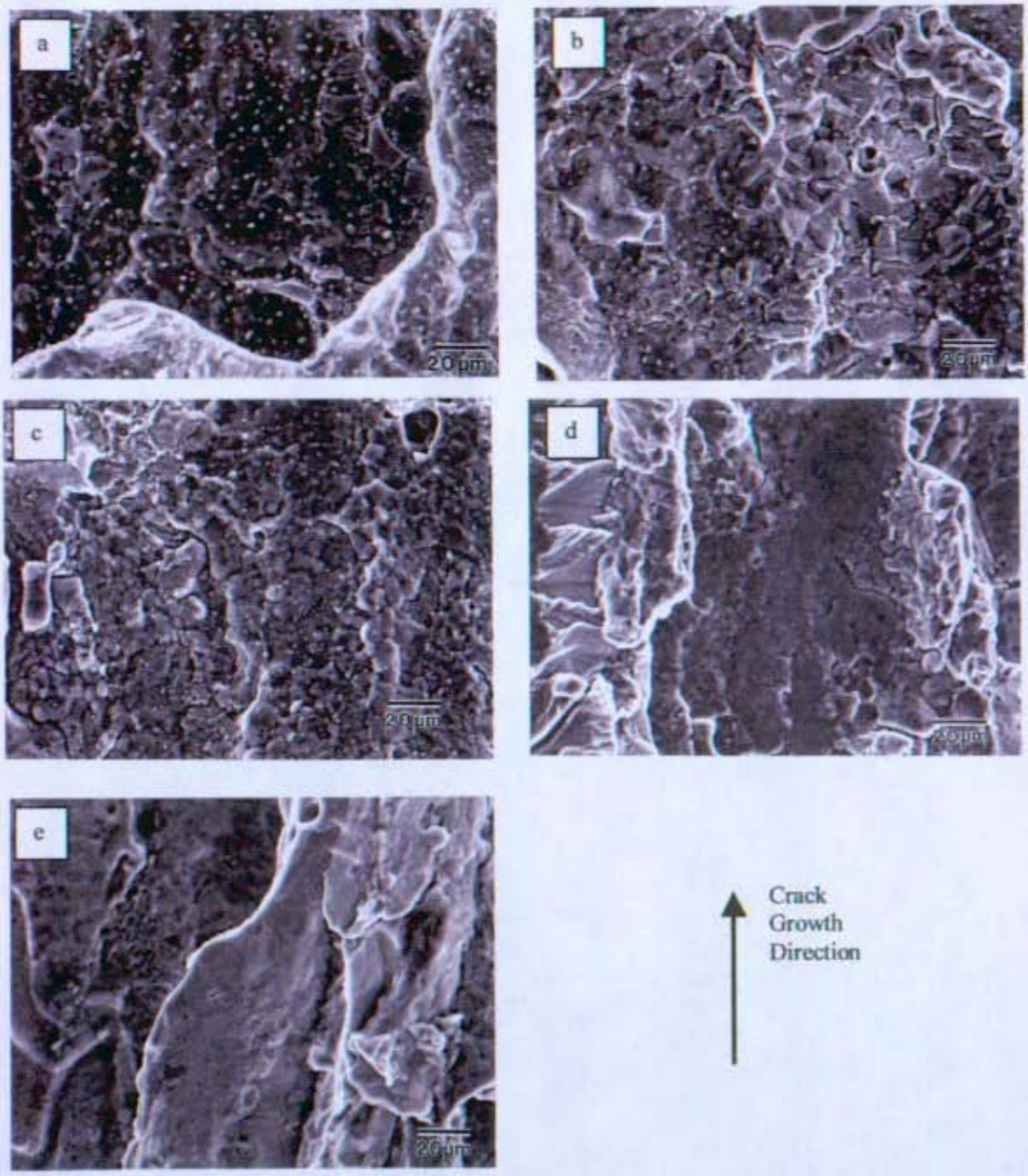

Figure 10. *Comparison of HEAC regions of each alloy and temper investigated in this study. The light particles in the copper bearing alloy (a, b, and c) were identified as S-phase. The fracture surface from 60 °C, 90% RH air tests are shown for a) AA 7050 UA, b) AA 7050 PA, c) AA 7050 OA, d) low Cu PA, and e) low Cu OA.*

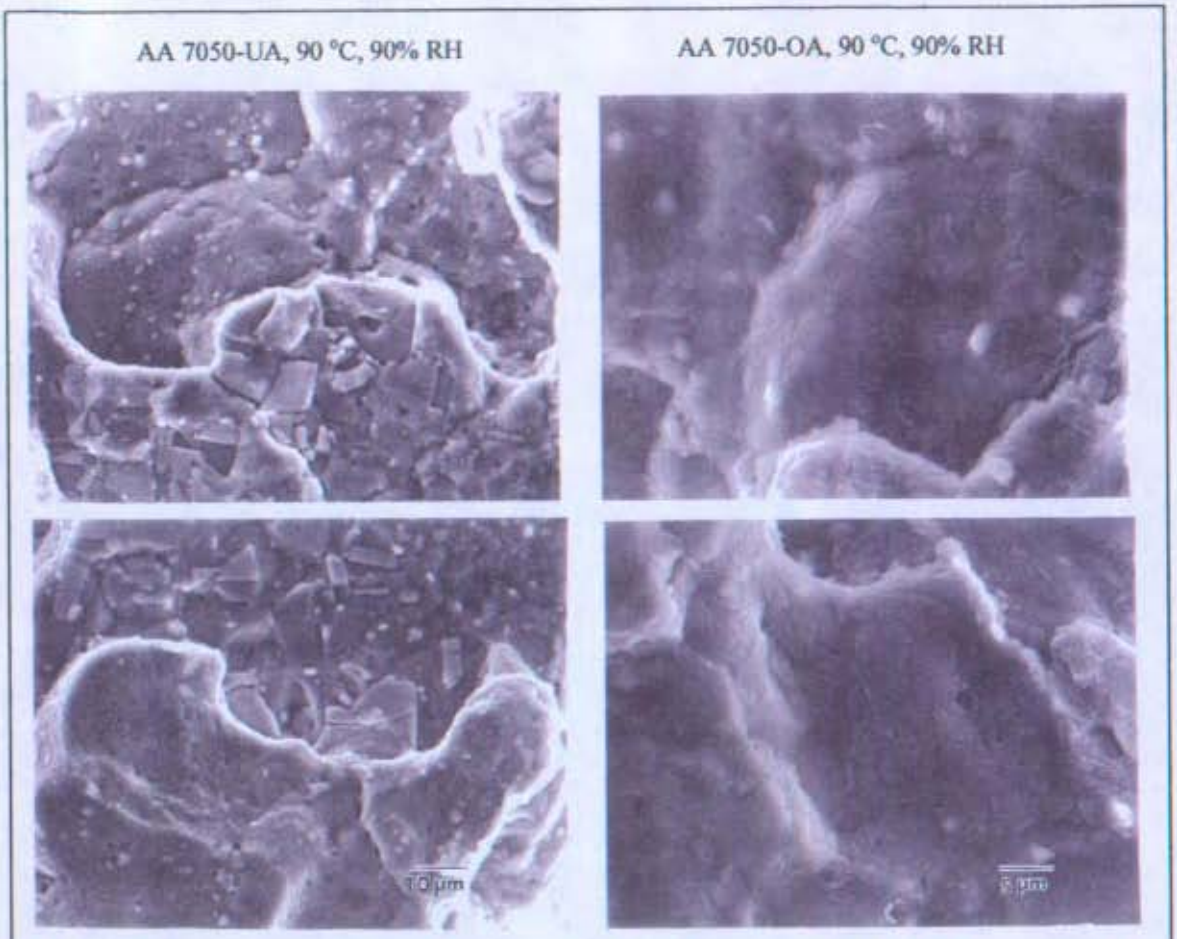

Figure 11. *Scanning electron micrographs showing matching halves fracture surfaces from the fastest cracking temper (AA 7050-UA, on the left) and the slowest cracking temper (AA 7050-OA, on the right). These fracture surfaces are from crack growth rate tests conducted in 90 °C, 90% RH air.*

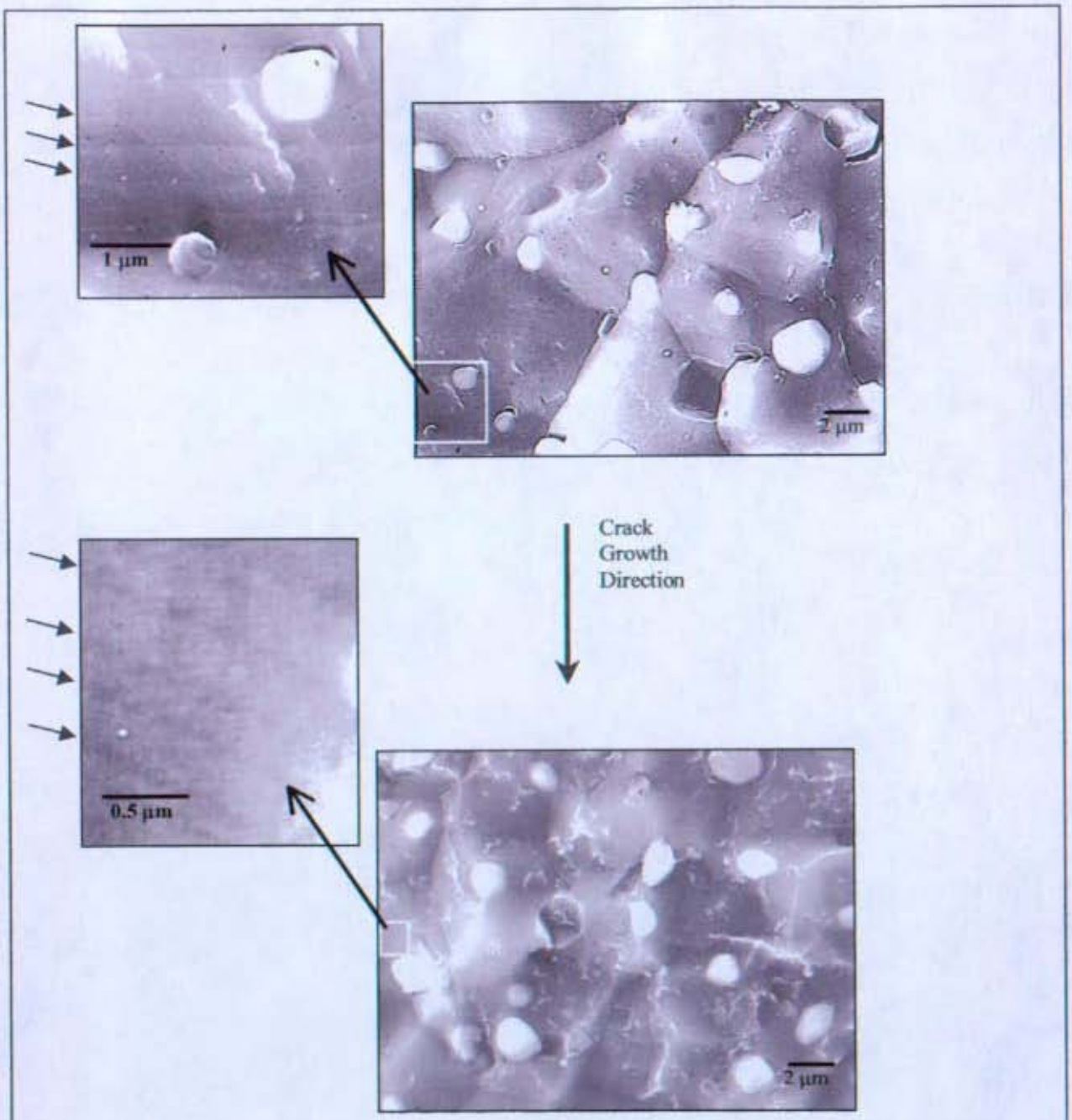

Figure 12. *Scanning electron fractographs for stabilized AA 7050 EAC surface produced in 60 °C, 90% humid air. Small black arrows indicate striation-type features observed at high magnification. The crack growth direction is from the top of the page to the bottom. Courtesy of L.M. Young [76].*